

Supporting Information

Table of Contents

| | |
|---|-----|
| 1. Experimental section..... | S2 |
| 1.1 General | S2 |
| 1.2 Synthetic procedures and characterization data..... | S2 |
| 1.3 OFET fabrication and characterization..... | S5 |
| 2. Additional spectra | S6 |
| 3. Theoretical calculations..... | S14 |
| 4. ^1H , ^{13}C NMR and HR mass spectra | S18 |
| 5. References..... | S24 |

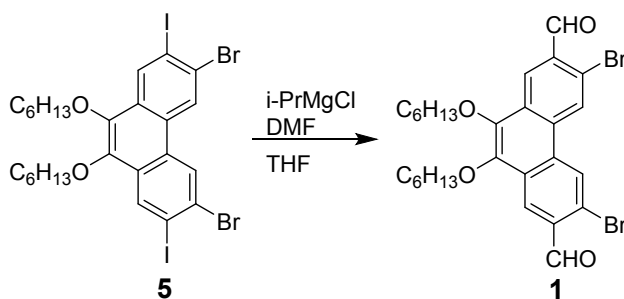
1. Experimental Section

1.1. General

All reagents and starting chemicals were obtained from commercial sources and used without further purification. Anhydrous 1, 2-dichloroethane was distilled from CaH₂. Anhydrous tetrahydrofuran (THF) were distilled from sodium-benzophenone immediately prior to use. Compounds **1**² and **2**² were prepared according to literature procedures. The UV-vis absorption spectra were conducted on a Shimadzu UV-1700/UV-3600 spectrometer. The photoluminescence (PL) spectra were performed using a Shimadzu RF-5301PC spectrofluorometer. The ¹H NMR and ¹³C NMR spectra were recorded in solution of CDCl₃/Toluene-*d*₈ on Bruker DPX400/DPX500 NMR spectrometer with tetramethylsilane (TMS) as the internal standard. The following abbreviations were used to explain the multiplicities: s = singlet, d = doublet, t = triplet, m = multiplet. MALDI-TOF mass spectra (MS) were recorded on a Bruker amazon instrument.

1.2. Synthetic procedures and characterization data

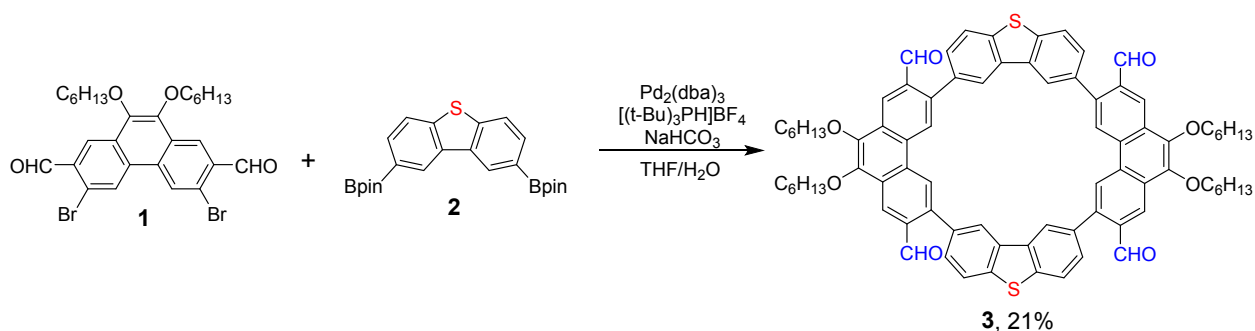
Synthesis of compound **1**.



Compound **1**¹ was synthesized by slight modification of the literature procedure. To a nitrogen purged solution of **5**¹ (2.80 g, 3.55 mmol) in THF (120 mL) at 0 °C was added dropwise a solution of isopropylmagnesium chloride (3.91 mL, 7.82 mmol, 2 M solution in THF). After addition, the mixture was kept stirring for additional 30 minutes at 0 °C. Then, anhydrous DMF (0.68 mL, 8.88 mmol) was added dropwise and the reaction mixture was warmed up to ambient temperature and stirred for 3 hours. Aqueous ammonium chloride solution was added, the mixture was extracted with DCM. The organic layer was washed with brine and dried over anhydrous sodium sulfate. The solvent was removed under reduced pressure and the residue was purified by flash column chromatography (silica gel, DCM/Hexane = 1:1). Yellow solid **1** was obtained in 63% yield (1.33 g). ¹H NMR (400 MHz, CDCl₃, δ ppm): 10.53 (s, 2H), 8.79 (s, 2H),

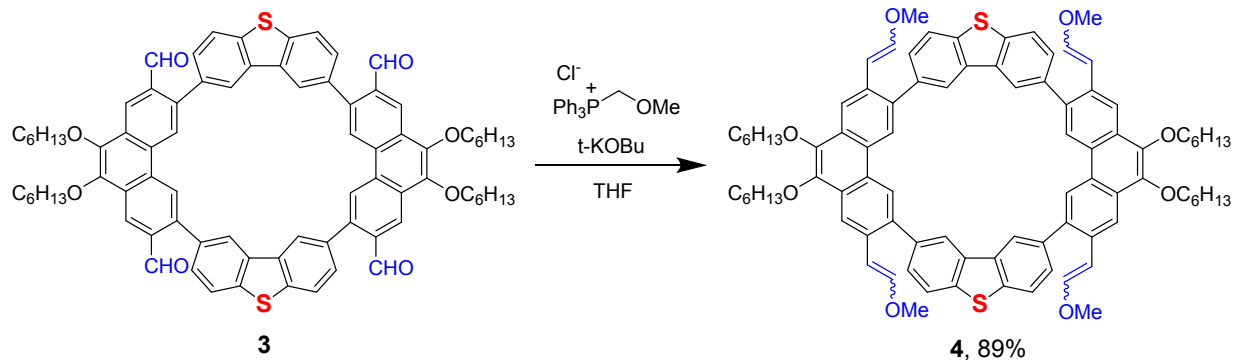
8.76 (s, 2H), 4.22 (t, 4H, $J = 6.7$ Hz), 1.94-1.87 (m, 4H), 1.57-1.54 (m, 4H), 1.39-1.37 (m, 8H), 0.93 (t, 6H, $J = 6.8$ Hz). ^{13}C NMR (100 MHz, CDCl_3 , δ ppm): 191.35, 144.00, 132.41, 131.16, 130.53, 128.70, 125.80, 122.28, 74.15, 31.63, 30.24, 25.79, 22.62, 14.01. MALDI-TOF Mass: m/z 592.0, calc. 592.1.

Synthesis of macrocycle **3** by Suzuki coupling reaction.



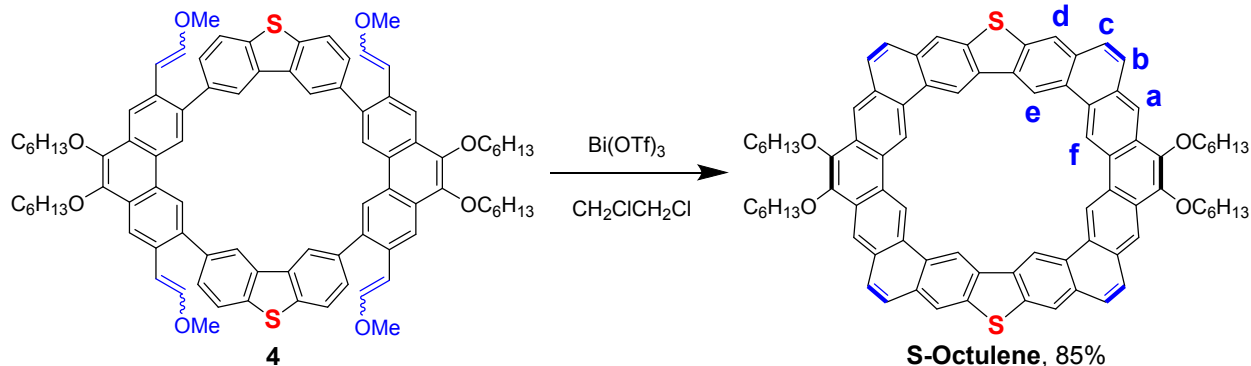
A mixture of **1** (220 mg, 0.37 mmol), **2** (163 mg, 0.37 mmol), NaHCO_3 (1.5 g, 17.86 mmol), THF (250 mL) and H_2O (15 mL), was carefully degassed before $\text{Pd}_2(\text{dba})_3$ (34 mg, 0.037 mmol), and $[(t\text{-Bu})_3\text{PH}]\text{BF}_4$ (43 mg, 0.149 mmol) were added. The mixture was stirred and heated at 80°C under nitrogen atmosphere for 2 days. The organic solvent was removed under reduced pressure, then H_2O and DCM were added. The organic layer was separated, dried over anhydrous sodium sulfate, and evaporated to dryness. The residue was first purified by a short column chromatography (silica gel, DCM/Hexane = 2:1) to remove catalysts, and then further purified on by preparative GPC using CHCl_3 at a rate of 14 mL/min. Yellow solid macrocycle **3** was obtained in 21% yield (48 mg). ^1H NMR (500 MHz, CDCl_3 , δ ppm): 10.20 (s, 4H), 9.00 (s, 4H), 8.85 (s, 4H), 8.59 (d, 4H, $J = 1.4$ Hz), 7.97 (d, 4H, $J = 8.3$ Hz), 7.47-7.45 (m, 4H), 4.37-4.30 (m, 8H), 2.01-1.95 (m, 8H), 1.64-1.59 (m, 8H), 1.44-1.38 (m, 16H), 0.94 (t, 12H, $J = 7.1$ Hz). ^{13}C NMR (100 MHz, CDCl_3 , δ ppm): 191.82, 144.08, 141.45, 139.98, 135.90, 135.08, 133.22, 130.84, 130.59, 130.17, 126.17, 124.26, 122.46, 122.29, 74.16, 31.73, 30.40, 25.91, 22.69, 14.08. MALDI-TOF Mass: m/z 1228.5, calc. 1228.5.

Synthesis of precursor **4**.



Under nitrogen atmosphere, to a solution of methoxymethyltriphenyl-phosphonium chloride (89 mg, 0.26 mmol) in THF (20 mL) at 0 °C was added t-BuOK (30 mg, 0.26 mmol). After stirring for 30 mins, a solution of **3** (40 mg, 0.033 mmol) in THF (10mL) was added and stirred at 25 °C for 2 h. The reaction solution was quenched by water and extracted by DCM. The organic layer was dried over Na₂SO₄ and the solvent was removed under reduced pressure. The residue was purified by flash column chromatography (silica gel, DCM/Hexane = 1:1). Yellow solid precursor **4** was obtained in 89% yield (39 mg). ¹H NMR (500 MHz, CDCl₃, δ ppm): 9.07 (d, 2H, *J* = 2.0 Hz), 8.60-8.57 (m, 4H), 8.40-8.39 (m, 2H), 8.29 (s, 2H), 7.90-7.87 (m, 4H), 7.54-7.50 (m, 4H), 7.17-7.14 (m, 2H), 6.21-6.19 (m, 2H), 5.89-5.86 (m, 4H), 5.33-5.30 (m, 2H), 4.32-4.29 (m, 8H), 3.87 (s, 6H), 3.56 (s, 6H), 1.99-1.95 (m, 8H), 1.70-1.63 (m, 8H), 1.64-1.40 (m, 16H), 0.97-0.95 (m, 12H). ¹³C NMR (125 MHz, CDCl₃, δ ppm): 149.46, 148.59, 143.64, 143.54, 143.20, 143.10, 138.81, 138.54, 138.50, 138.41, 136.05, 135.98, 133.35, 132.10, 129.62, 129.46, 129.06, 128.85, 126.89, 126.46, 124.31, 122.74, 122.51, 121.76, 117.72, 104.51, 103.71, 73.76, 73.68, 60.81, 56.46, 56.43, 31.97, 31.82, 30.68, 30.65, 30.61, 30.59, 26.16, 25.98, 22.77, 22.71, 14.16, 14.11. MALDI-TOF Mass: *m/z* 1340.7, calc. 1340.6.

Synthesis of heterocycloarene S-Octulene.



Under nitrogen atmosphere, $\text{Bi}(\text{OTf})_3$ (13 mg, 0.020 mmol) was added to the 20 ml dry $\text{CH}_2\text{ClCH}_2\text{Cl}$ solution of compound **4** (35 mg, 0.026 mmol), and the solution was stirred at room temperature for 3 h. The reaction solvent was removed under reduced pressure. The residue was purified by flash column chromatography (silica gel, DCM/Hexane = 1:1). Yellow solid heterocycloarene **S-Octulene** was obtained in 85% (27 mg). ^1H NMR (400 MHz, CDCl_3 , δ ppm): 9.60 (s, 4H), 9.41 (s, 4H), 8.57 (s, 4H), 7.92 (s, 4H), 7.69 (d, 4H, $J = 8.8$ Hz), 7.47 (d, 4H, $J = 8.9$ Hz), 4.14 (t, 8H, $J = 6.6$ Hz), 1.87-1.80 (m, 8H), 1.50-1.48 (m, 8H), 1.36-1.34 (m, 16H), 0.95-0.92 (m, 12H). ^{13}C NMR (100 MHz, CDCl_3 , δ ppm): 141.39, 139.27, 135.09, 131.37, 130.86, 130.07, 129.34, 129.16, 128.81, 127.84, 126.82, 122.41, 122.25, 118.43, 117.98, 73.23, 31.77, 30.50, 25.94, 22.71, 14.12. MALDI-TOF Mass: m/z 1213.5, calc. 1213.5. HRMS (APCI, m/z): $[(\text{M}+\text{H})^+]$ calcd for $\text{C}_{84}\text{H}_{77}\text{O}_4\text{S}_2$, 1213.5258; found, 1213.5254.

1.3. OFET fabrication and characterization

The SiO_2/Si wafers used in this work were rinsed with deionized water, hot piranha solution ($\text{H}_2\text{SO}_4/\text{H}_2\text{O}_2 = 2:1$), deionized water, ethanol, and finally were dried in an oven at 70°C . For the octadecyltrichlorosilane surface modification, a small drop of OTS surrounded by those cleaned SiO_2/Si substrates were put into a Petri dish. Then the dish was placed into a vacuum oven and kept at 120°C for 3 hours. When the temperature returned to approximately room temperature, OTS self-assembled monolayer was formed on the surface of the SiO_2/Si wafers. Those OTS modified wafers should be washed immediately in turn by hexane, ethanol, and chloroform and finally were blown dry with high-purity nitrogen gas.

The bottom-gate bottom-contact (BGBC) devices were fabricated by spin-coating on the OTS modified SiO₂/Si substrates. The gold source/drain electrodes were sputtered and patterned on the substrates by photolithography technique before rinsing process. The Sulfur-Heterooctene dissolved in hot dimethyl sulfoxide was spun with speed of 3000 rpm for 60 seconds. The annealing process was carried out in a vacuum oven at 200 °C for 30 minutes before electrical measurements. In addition, the semiconductor layer was also prepared by drop casting with chloroform as solvent. The solution with a 1:1 mixture of **S-Octulene** and fullerenes, including C₆₀ and C₇₀ respectively, was also dropped for semiconductor layers preparation. What's more, the bottom-gate top-contact (BGTC) configuration OFETs were also fabricated by vapor deposition of gold source/drain electrodes onto the semiconductor layer through a shadow mask with the channel length was 10 μm and the channel width was 100 μm.

OFET devices characterizations were carried out at room temperature using a Keithley 4200 in ambient air. The mobilities were calculated in the saturation by the equation:

$$I_{DS} = \frac{W}{2L} C_i \mu (V_{GS} - V_T)^2$$

where I_{DS} is the drain-source current, μ is the field-effect mobility, V_G is the gate voltage, V_T is the threshold voltage, W is the channel width, L is the channel width length, C_i is the capacitance of the insulating layer. In this work, the 300 nm SiO₂ surface layer with the capacitance of 11 nF/cm² was employed as the dielectric. OFET characteristics were obtained by applying a gate voltage from -60 V to 10 V, with the drain-source voltage kept at -60 V.

2. Additional spectra

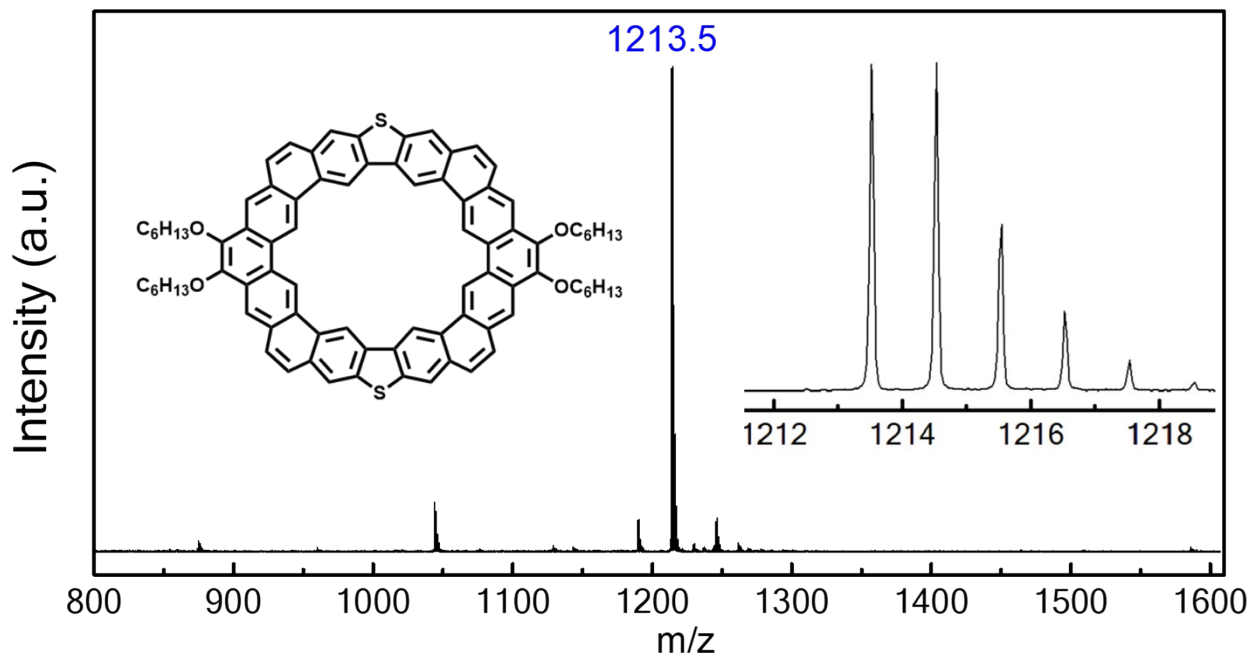


Figure S1. MALDI-TOF mass spectrum data for S-Octulene.

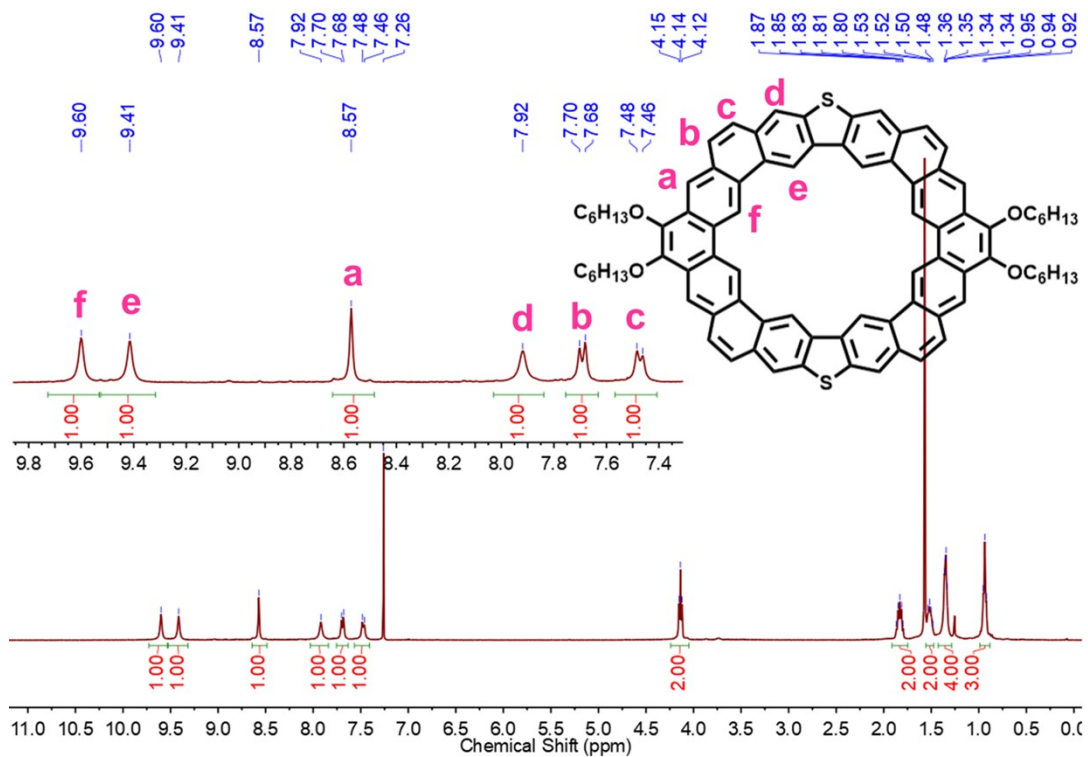


Figure S2. ^1H NMR spectrum of **S-Octulene** in CD_3Cl (400 MHz).

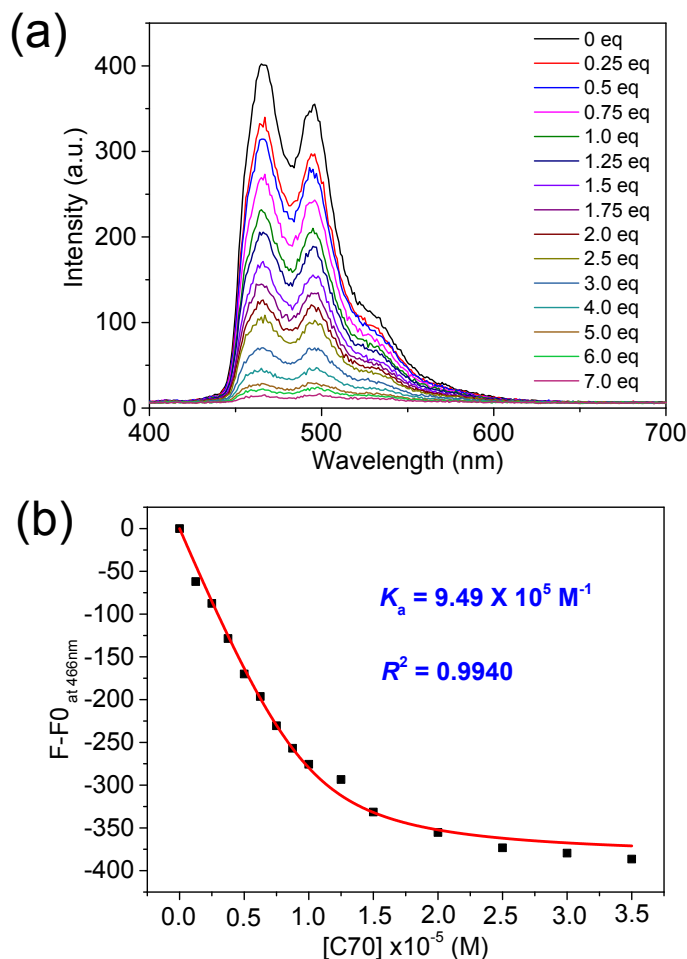


Figure S3. (a) Change of the fluorescence spectrum of **S-Octulene** upon gradual addition of **C₇₀** in toluene. (b) Plot of fluorescence changes at 466 nm versus $[\text{C}_{70}]$ in toluene for obtaining K_a , R^2 is the coefficient of determination.

Fluorescence titrations were carried out by adding stock toluene solutions of **C₆₀** ($1.5 \times 10^{-3} \text{ M}$) and **C₇₀** ($1.5 \times 10^{-3} \text{ M}$) to the solution of **S-Octulene** ($1.0 \times 10^{-5} \text{ M}$), respectively. **S-Octulene** giving a QY of 1.2% in toluene-ethanol solution with rhodamine B as a standard. QYs were calculated using rhodamine B in ethanol (QY = 0.89) with an absorbance of 0.01 at 480 nm as a reference (*Anal. Bioanal. Chem.* 2014, **407**, 59).

Estimation of the binding constant K_a in toluene:

Solution of C60 or C70 in toluene was added to a solution of **S-Octulene** at 25 °C. The change in the fluorescence at 466 nm was monitored. The association constant K_a for the 1:1 complexes was derived by using the non-linear curve fitting based on the equation:

$$\Delta A = \Delta A_{\infty} \left(\frac{(1 + K_a[G] + K_a[H]_0) - \left((1 + K_a[G] + K_a[H]_0)^2 - 4 K_a^2[H]_0[G] \right)^{0.5}}{2K_a[H]_0} \right)$$

Where $\Delta A = A - A_0$, $\Delta A_{\infty} = A_{\infty} - A_0$, $[G]$ is [C60] or [C70], $[H]_0 = [\text{S-Octulene}]$.

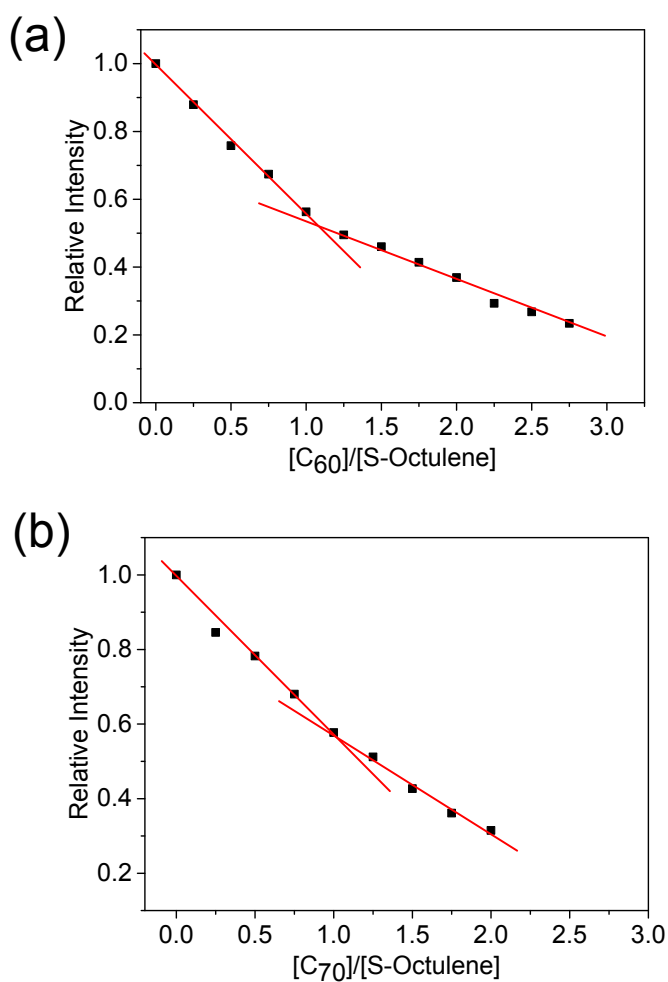


Figure S4. (a) Mole ratio plot for **S-Octulene** and C₆₀, showing a 1:1 complexation stoichiometry. (b) Mole ratio plot for **S-Octulene** and C₇₀, showing a 1:1 complexation stoichiometry

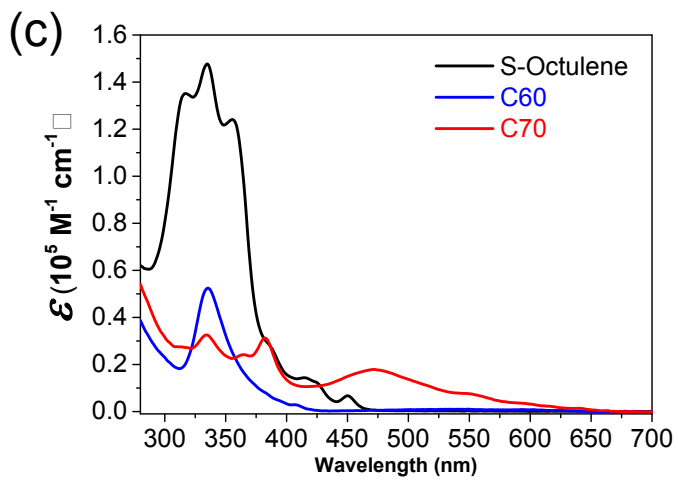
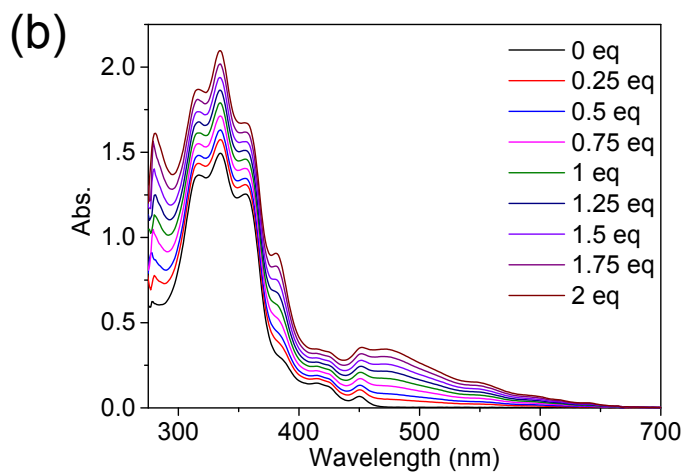
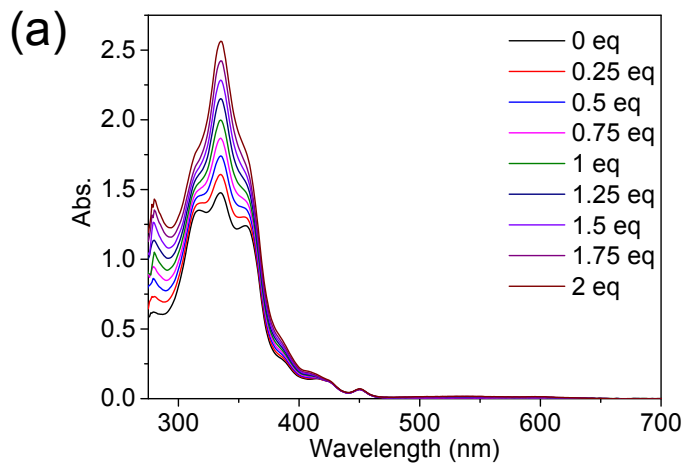


Figure S5. UV-Vis absorption spectra of **S-Octulene** in the presence of C_{60} (a) and C_{70} (b) in toluene. (c) Absorption spectra of **S-Octulene**, C_{60} and C_{70} in toluene. $[S\text{-Octulene}] = 1.0 \times 10^{-5}$ M, $[C_{60}] = [C_{70}] = 1.5 \times 10^{-3}$ M.

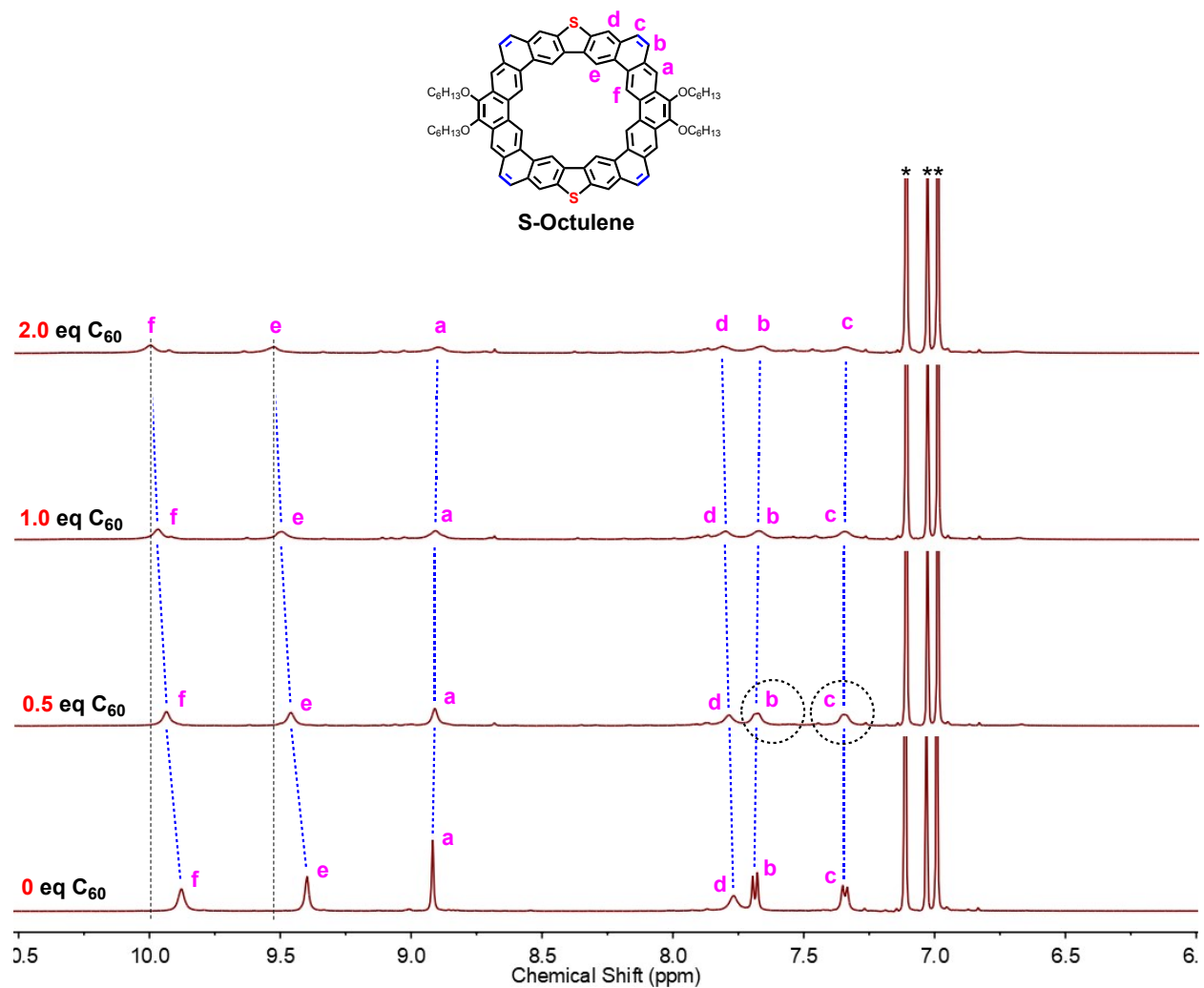


Figure S6. ^1H NMR spectral change of **S-Octulene** in toluene- d_8 with addition of C_{60} at 298 K; the peaks labeled by an asterisk indicate residue solvents. The concentration of **S-Octulene** is 4.3 mg/mL.

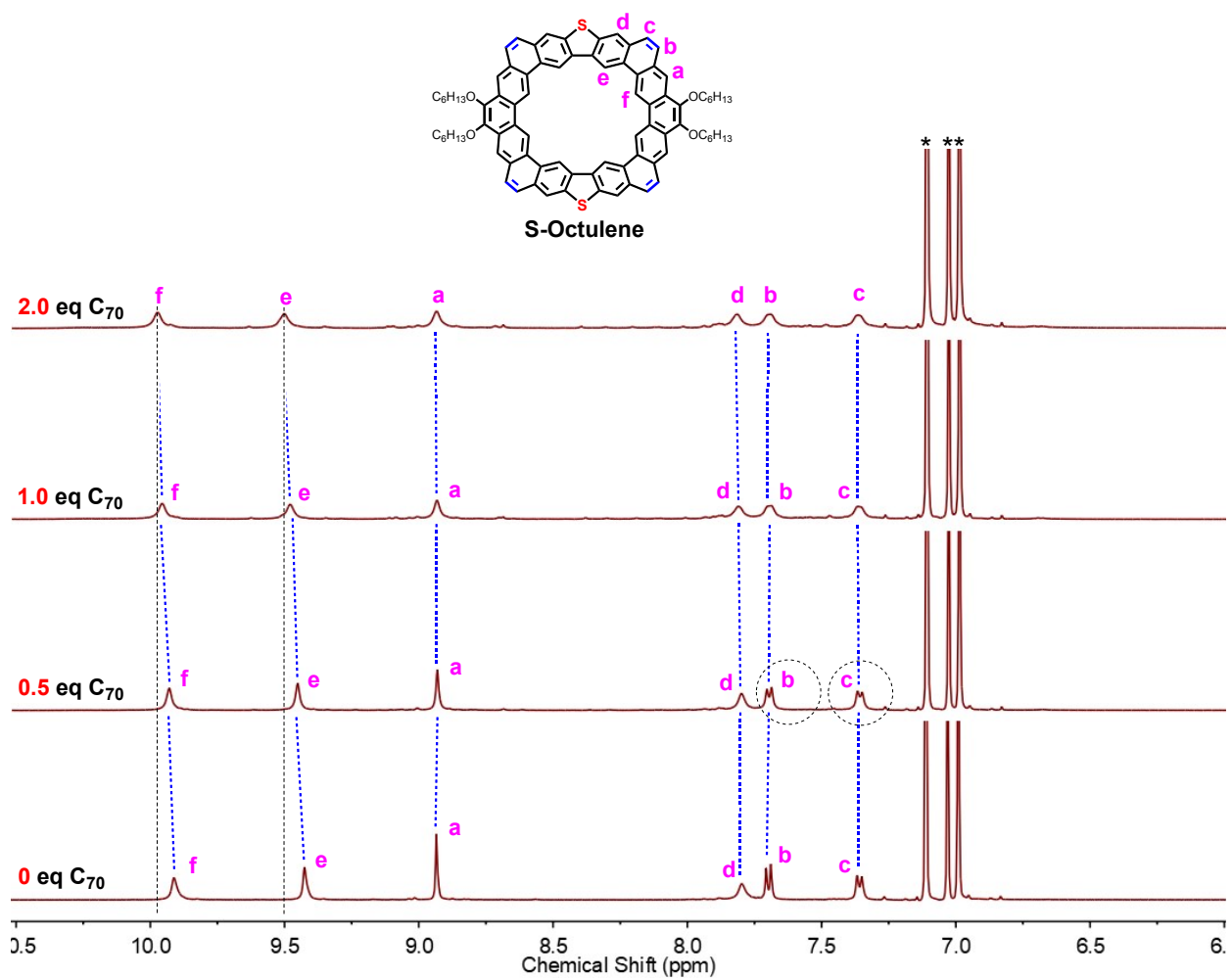


Figure S7. ¹H NMR spectral change of **S-Octulene** in toluene-*d*₈ with addition of C₇₀ at 298 K; the peaks labeled by an asterisk indicate residue solvents. The concentration of **S-Octulene** is 4.0 mg/mL.

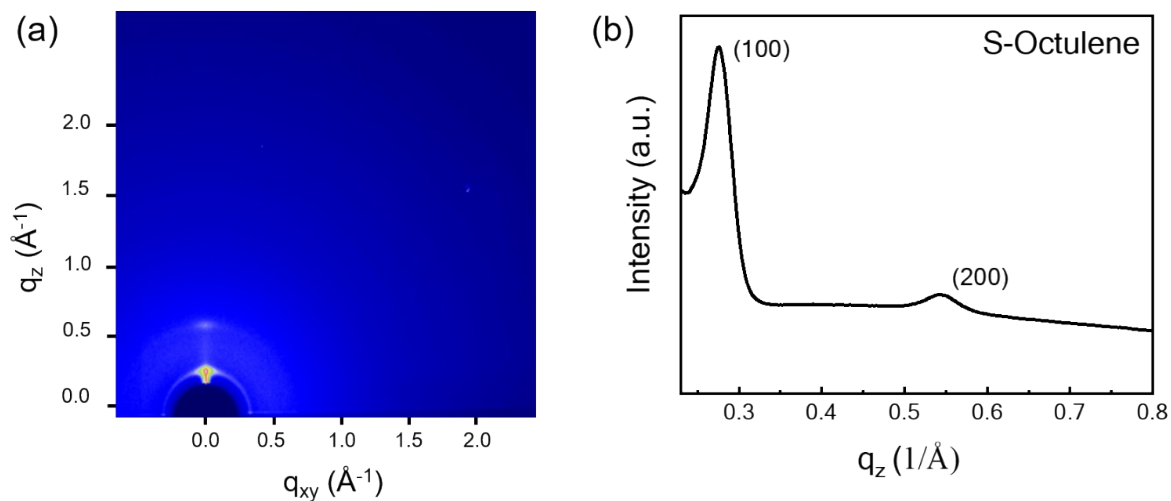


Figure S8. (a) 2D GI-XRD pattern of thin film based on **S-Octulene**. (b) Corresponding 1D GI-XRD profile of out-of-plane for **S-Octulene**. Exhibiting the out-of-plane packing peaks with a packing distance of 22.75 Å, which is larger than the simulated value as the presence of the side chain.

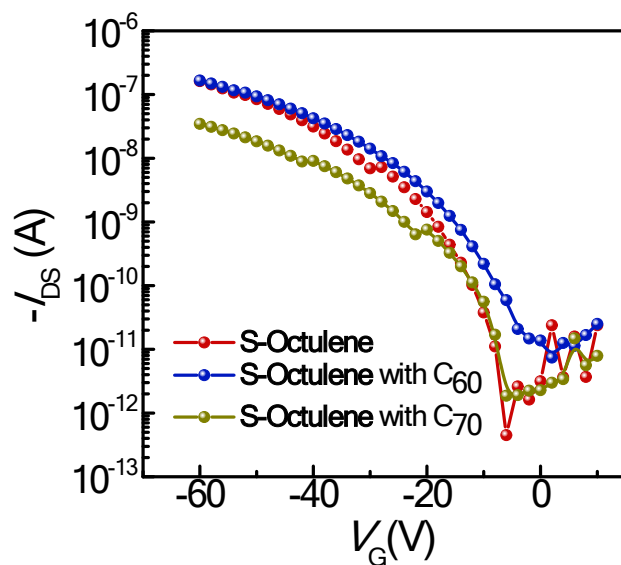


Figure S9. Representative transfer curves of OFETs fabricated with **S-Octulene**, **S-Octulene** with C_{60} and C_{70} .

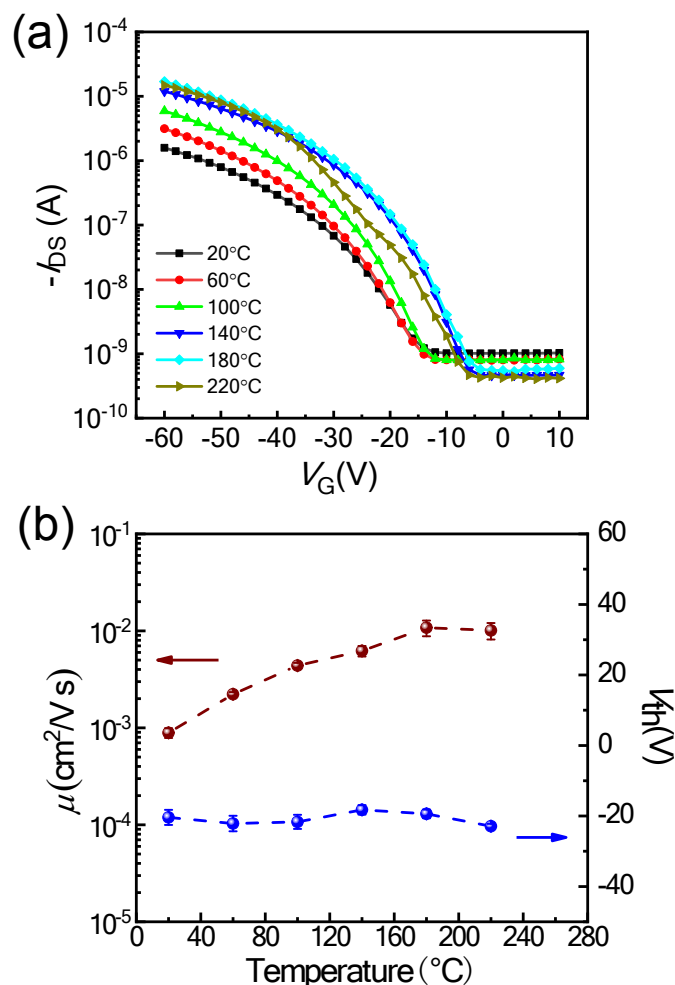


Figure S10. (a) Transfer curves of **S-Octulene** at different temperature. (b) Measured mobilities and threshold voltage calculated from the transfer curves.

3. Theoretical calculations

Theoretical calculations were performed with the Gaussian09 program suite.³ All calculations were carried out using the density functional theory (DFT) method with Becke's threeparameter hybrid exchange functionals and the Lee-Yang-Parr correlation functional (B3LYP) employing the 6-31G(d,p) basis set for all atoms.⁴ Time-dependent DFT (TD-DFT) calculations have been conducted under same level of theory and basis set with PCM model as solvation of dichloromethane. NICS values of 1b was calculated by GIAO procedure (NMR pop=NCSall)⁵ under same level of theory and basis set based on the optimized structure with the assistance of Multiwfn.⁶ ACID plot was calculated by using the method developed by Herges.⁷

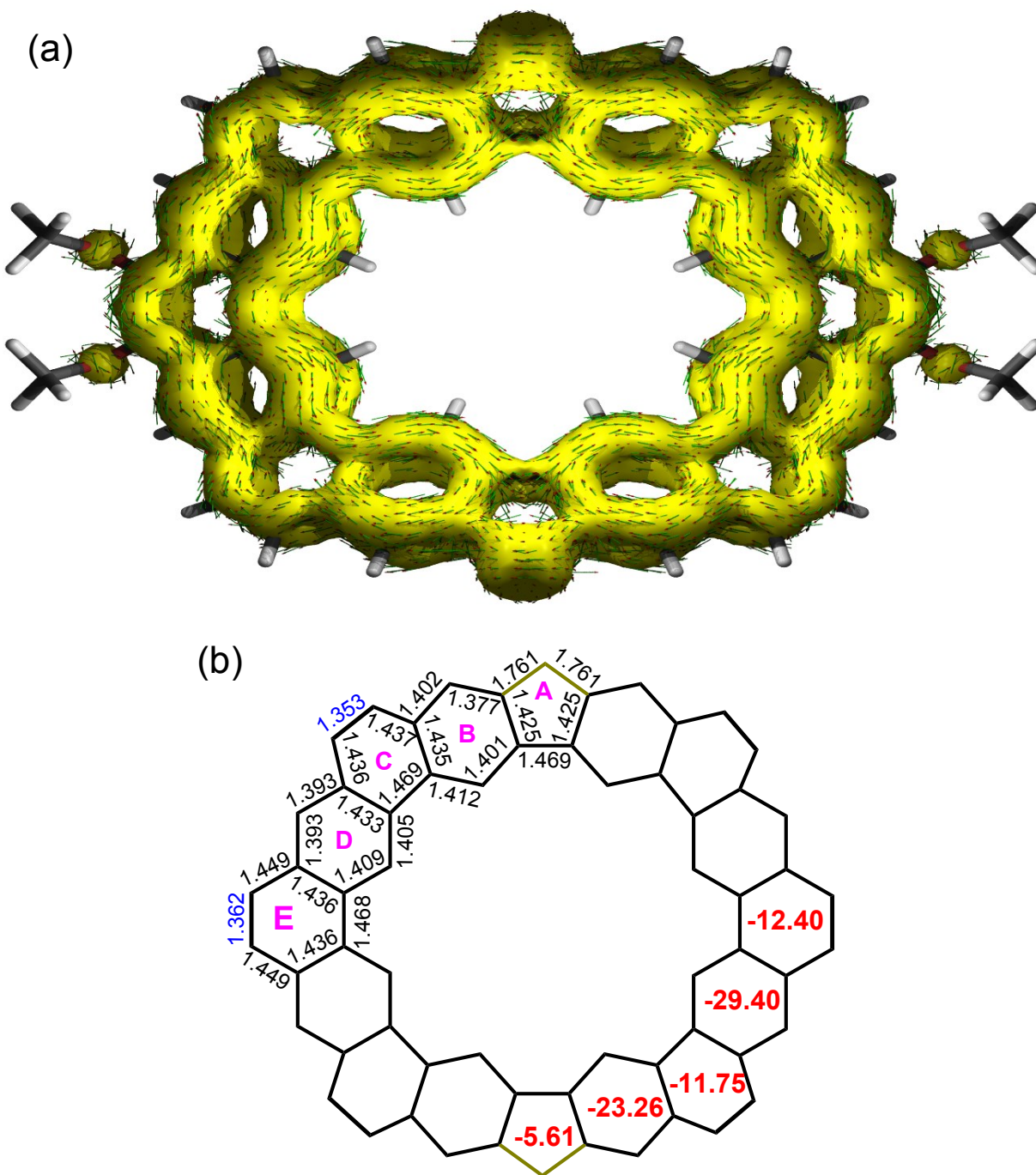


Figure S11. (a) Calculated (RB3LYP/6-31G (d,p)) ACID plot (contribution from π electrons only) of **S-Octulene**, The magnetic field is perpendicular to the XY plane and points out through the paper. (b) Calculated (RB3LYP/6-31G (d,p)) bond lengths (in Å) of the backbone for the **S-Octulene**. The red numbers in the rings are the calculated NICS(1)zz values -1 Å. Both of the NICS(1)zz values +1 Å and -1 Å for each rings show the same aromaticity trend.

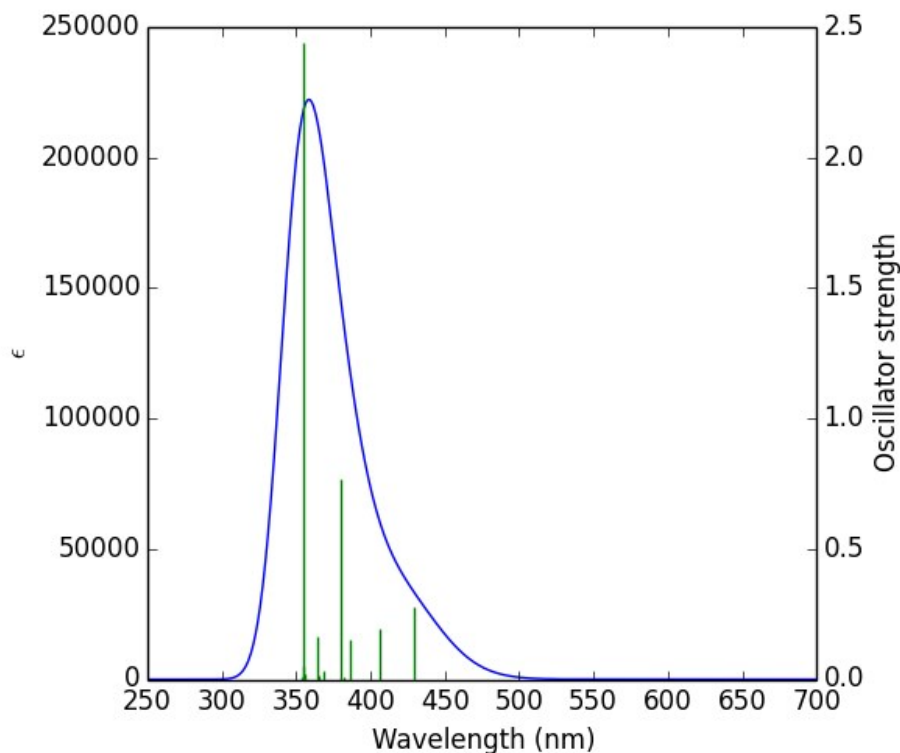


Figure S12. TD DFT simulated spectrum of **S-Octulene** in DCM.

Table S1. Selected TD-DFT (RB3LYP/6-31G*) calculated energies, oscillator strength and compositions of major electronic transitions of **S-Octulene**.

| Wavelength (nm) | Osc.Strength (f) | Major contributions |
|-----------------|------------------|---|
| 461.11 | 0.0 | HOMO → LUMO (95%) |
| 445.36 | 0.0 | HOMO-1 → LUMO (85%), HOMO → LUMO+2 (8%) |
| 429.80 | 0.2769 | HOMO-2 → LUMO (78%), HOMO-3 → LUMO+2 (4%), HOMO-1 → LUMO+3 (8%), HOMO → LUMO+4 (7%) |
| 406.56 | 0.1956 | HOMO-3 → LUMO (70%), HOMO-1 → LUMO+1 (10%), HOMO-2 → LUMO+2 (8%), HOMO-1 → LUMO+4 (4%), HOMO → LUMO+3 (4%) |
| 387.78 | 0.0 | HOMO-2 → LUMO+4 (16%), HOMO-1 → LUMO+2 (75%), HOMO-2 → LUMO+1 (5%) |
| 386.68 | 0.1551 | HOMO-2 → LUMO (19%), HOMO-1 → LUMO+3 (36%), HOMO → LUMO+4 (28%), HOMO-5 → LUMO (5%), HOMO-3 → LUMO+2 (3%), HOMO → LUMO+1 (6%) |

| | | |
|--------|--------|---|
| 382.43 | 0.0 | HOMO-2 → LUMO+3 (22%), HOMO-1 → LUMO (13%), HOMO → LUMO+2 (58%), HOMO-3 → LUMO+4 (3%) |
| 382.40 | 0.0105 | HOMO-4 → LUMO (10%), HOMO-3 → LUMO (13%), HOMO-1 → LUMO+1 (68%), HOMO-1 → LUMO+4 (3%) |
| 380.40 | 0.0018 | HOMO-1 → LUMO+4 (12%), HOMO → LUMO+3 (69%), HOMO-4 → LUMO (2%), HOMO-3 → LUMO (9%), HOMO-2 → LUMO+2 (6%) |
| 379.83 | 0.7684 | HOMO → LUMO+1 (89%), HOMO → LUMO+4 (6%) |
| 371.12 | 0.0 | HOMO-2 → LUMO+1 (65%), HOMO-2 → LUMO+4 (11%), HOMO-1 → LUMO+2 (14%), HOMO → LUMO+5 (2%) |
| 368.55 | 0.0314 | HOMO-3 → LUMO+1 (11%), HOMO-2 → LUMO+3 (47%), HOMO → LUMO+2 (20%), HOMO-6 → LUMO (9%), HOMO-3 → LUMO+4 (4%), HOMO-1 → LUMO+5 (3%) |
| 365.41 | 0.0167 | HOMO-5 → LUMO (12%), HOMO-1 → LUMO+3 (49%), HOMO → LUMO+4 (35%) |
| 363.88 | 0.1621 | HOMO-4 → LUMO (51%), HOMO-1 → LUMO+1 (16%), HOMO-1 → LUMO+4 (21%), HOMO → LUMO+3 (10%) |
| 357.19 | 0.0 | HOMO-3 → LUMO+3 (43%), HOMO-2 → LUMO+1 (16%), HOMO-2 → LUMO+4 (29%), HOMO-7 → LUMO (2%), HOMO-1 → LUMO+2 (2%), HOMO → LUMO+5 (3%) |
| 356.31 | 0.0232 | HOMO-4 → LUMO (10%), HOMO-2 → LUMO+2 (58%), HOMO-1 → LUMO+4 (29%) |
| 355.40 | 0.0537 | HOMO-5 → LUMO (76%), HOMO → LUMO+4 (19%) |
| 354.64 | 2.4409 | HOMO-4 → LUMO (20%), HOMO-2 → LUMO+2 (27%), HOMO-1 → LUMO+4 (30%), HOMO → LUMO+3 (15%), HOMO-3 → LUMO (5%) |
| 354.19 | 0.0066 | HOMO-3 → LUMO+1 (64%), HOMO-2 → LUMO+3 (16%), HOMO-6 → LUMO (7%), HOMO → LUMO+2 (8%) |
| 345.99 | 0.0 | HOMO-3 → LUMO+3 (38%), HOMO-2 → LUMO+4 (40%), HOMO-5 → LUMO+1 (3%), HOMO-2 → LUMO+1 (6%), HOMO-1 → LUMO+2 (6%) |

4. ^1H , ^{13}C NMR and HR mass spectra

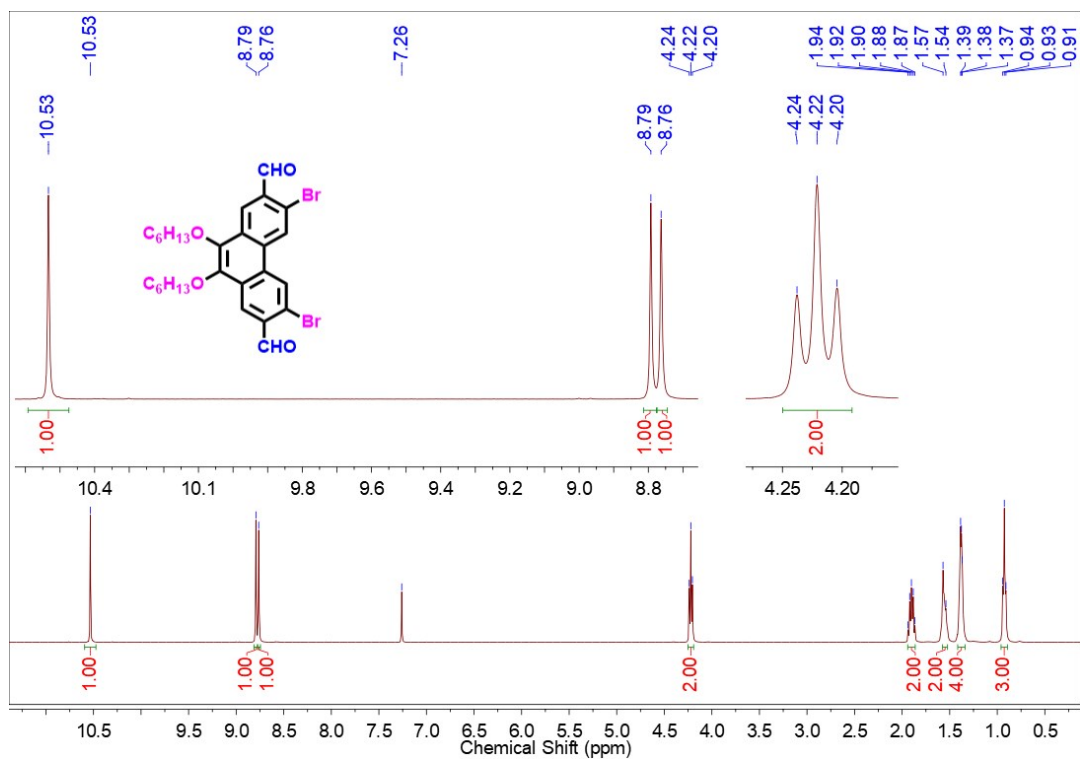


Figure S13. ^1H NMR spectrum (400 MHz) of **1** in CDCl_3 at 298 K.

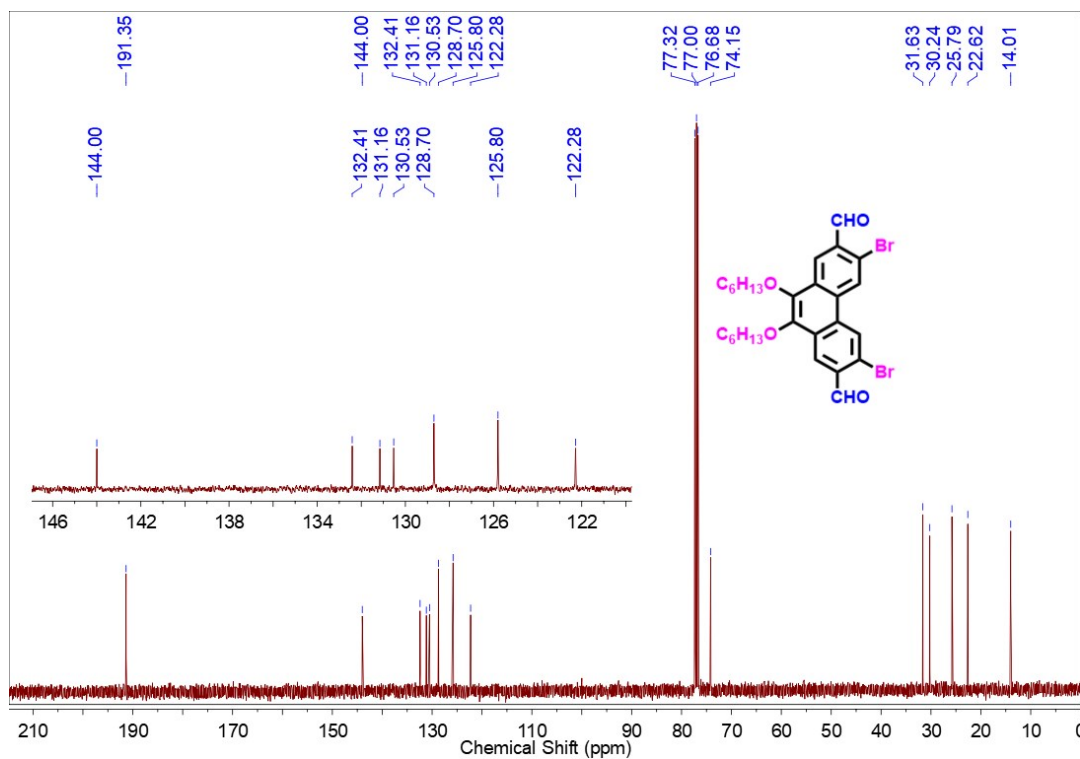


Figure S14. ^{13}C NMR spectrum (100 MHz) of **1** in CDCl_3 at 298 K.

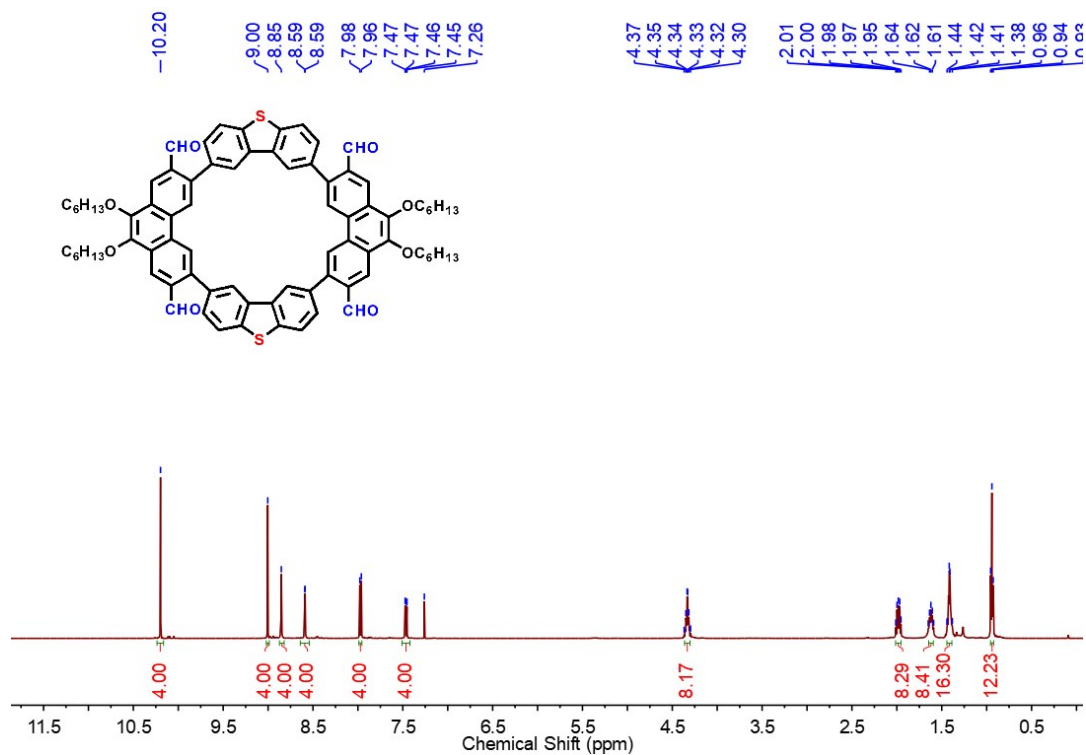


Figure S15. ^1H NMR spectrum (500 MHz) of **3** in CDCl_3 at 298 K.

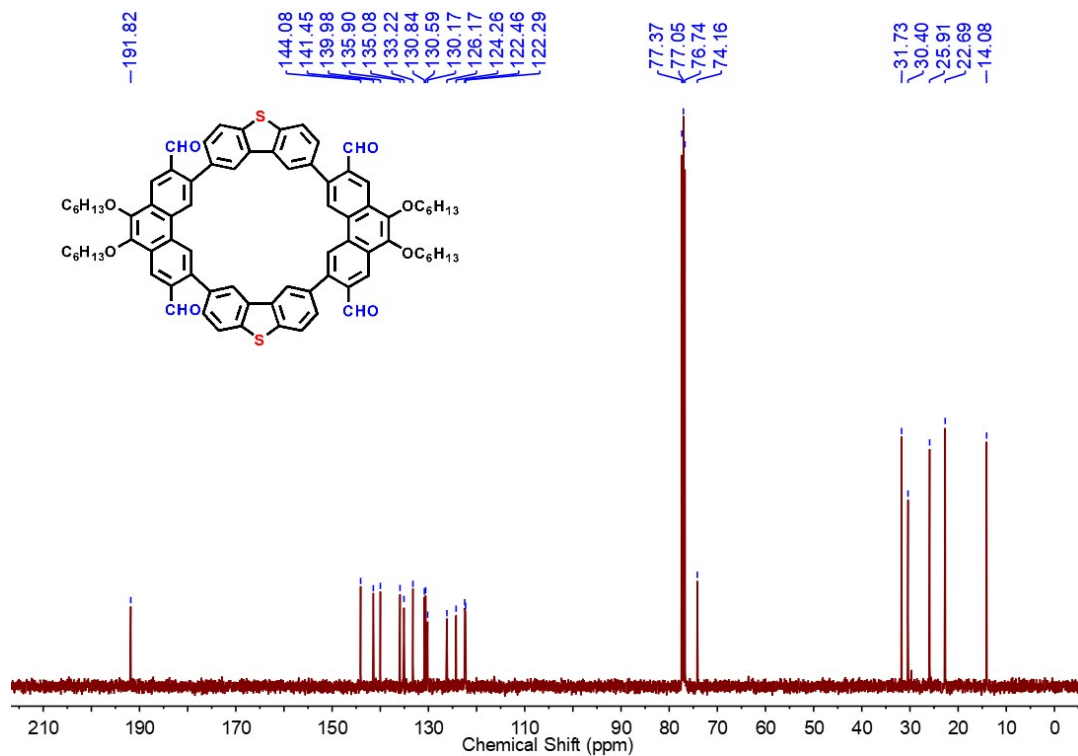


Figure S16. ^{13}C NMR spectrum (100 MHz) of **3** in CDCl_3 at 298 K.

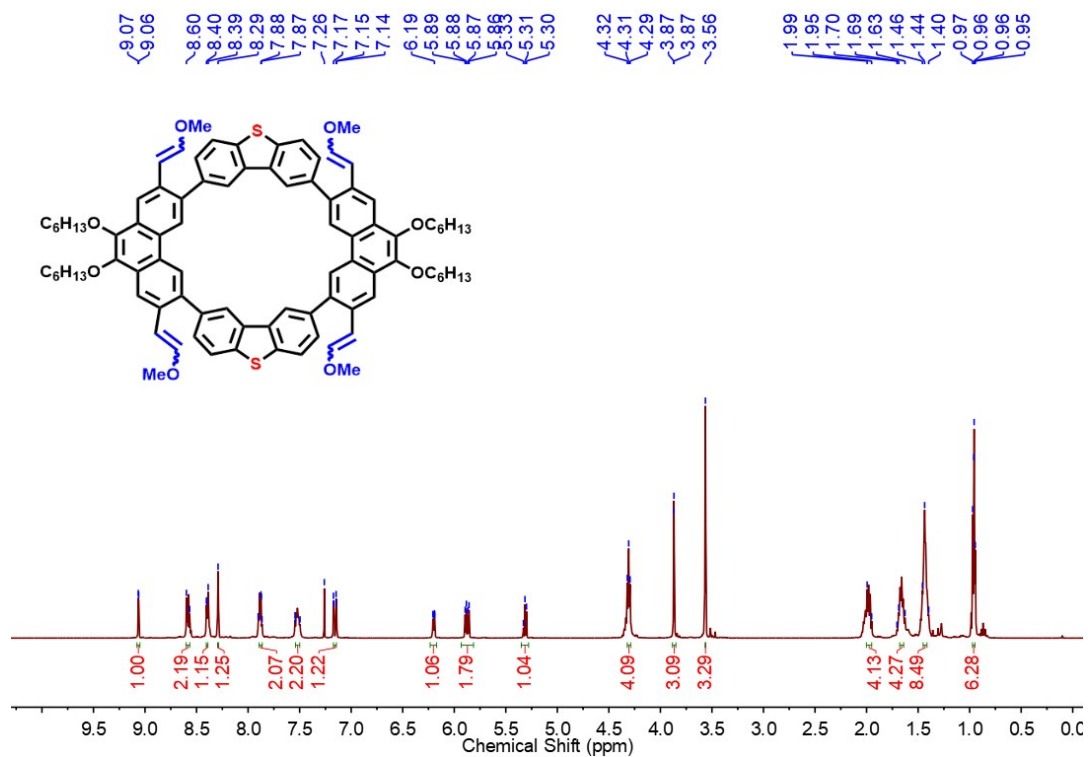


Figure S17. ¹H NMR spectrum (500 MHz) of 4 in CDCl₃ at 298 K.

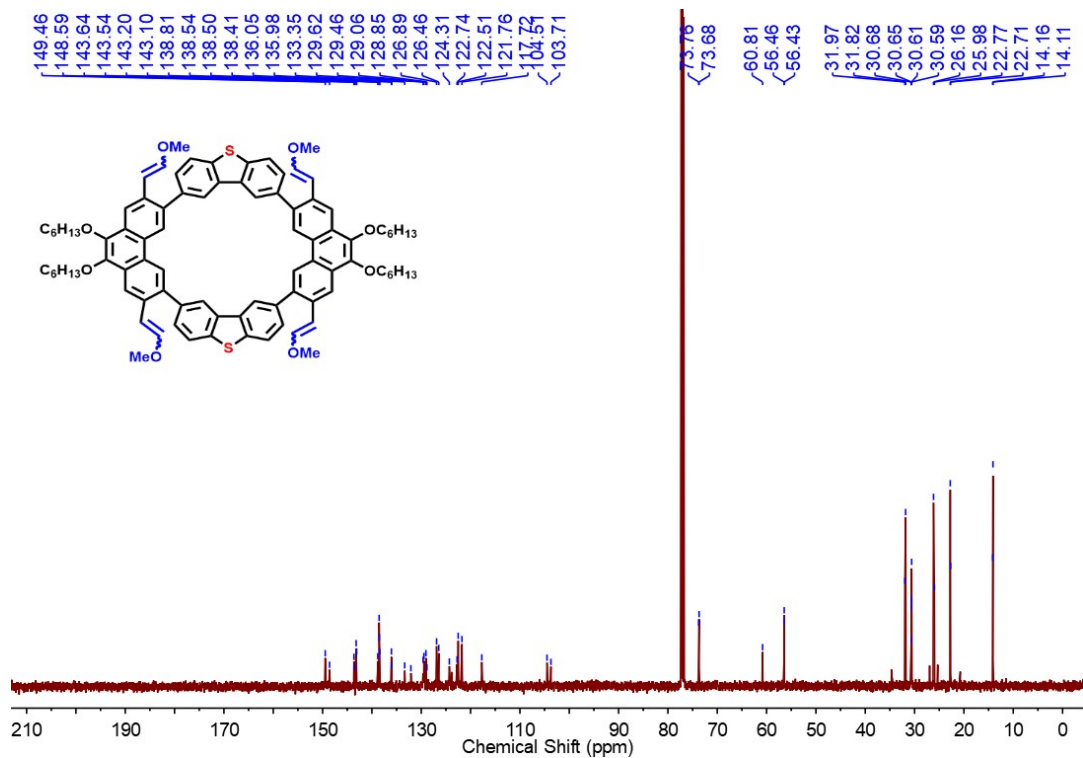


Figure S18. ¹³C NMR spectrum (125 MHz) of 4 in CDCl₃ at 298 K.

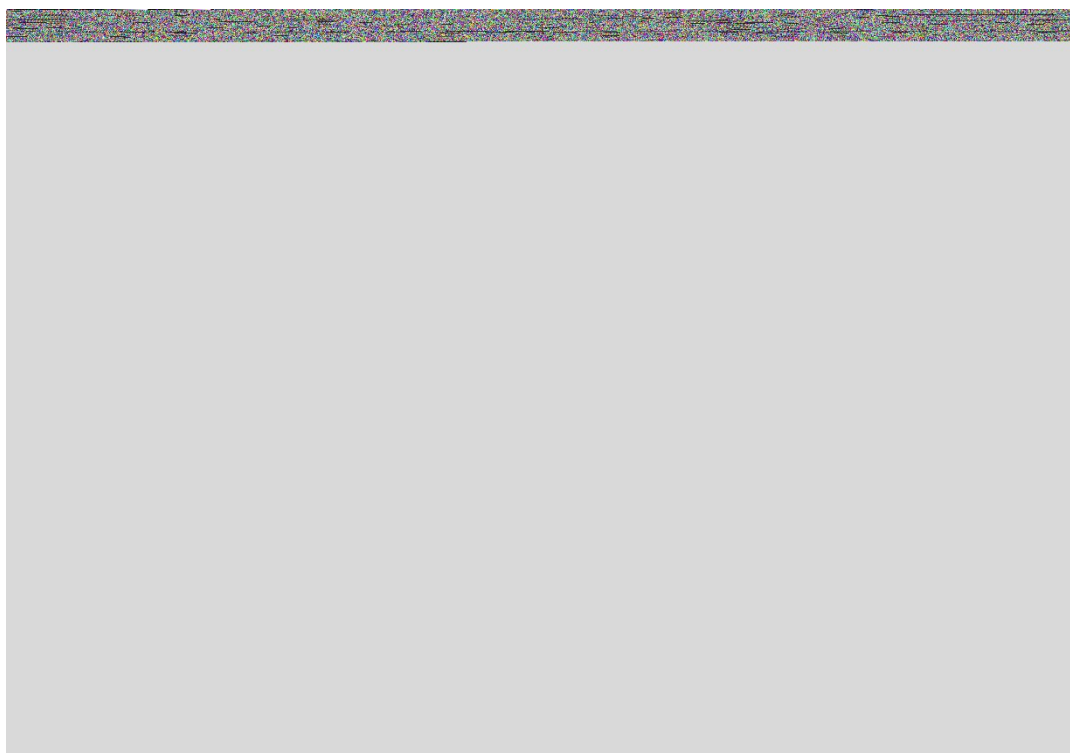


Figure S19. ^1H NMR spectrum (400 MHz) of **S-Octulene** in CDCl_3 at 298 K.

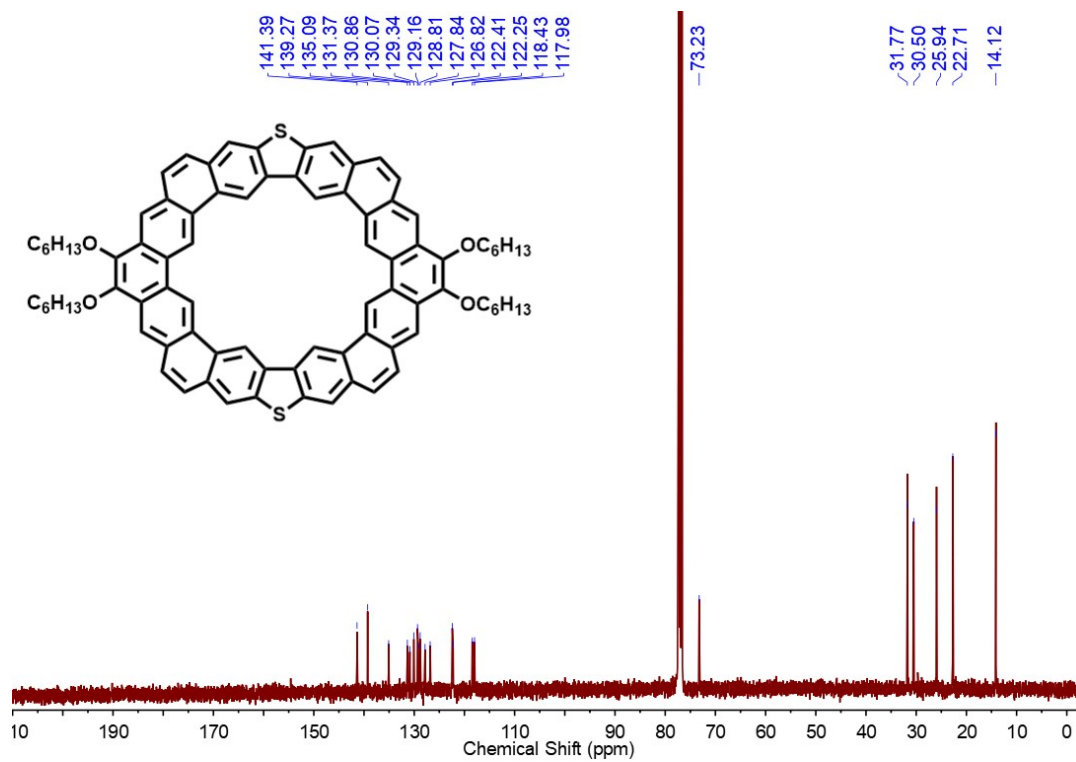


Figure S20. ^{13}C NMR spectrum (100 MHz) of **S-Octulene** in CDCl_3 at 298 K.

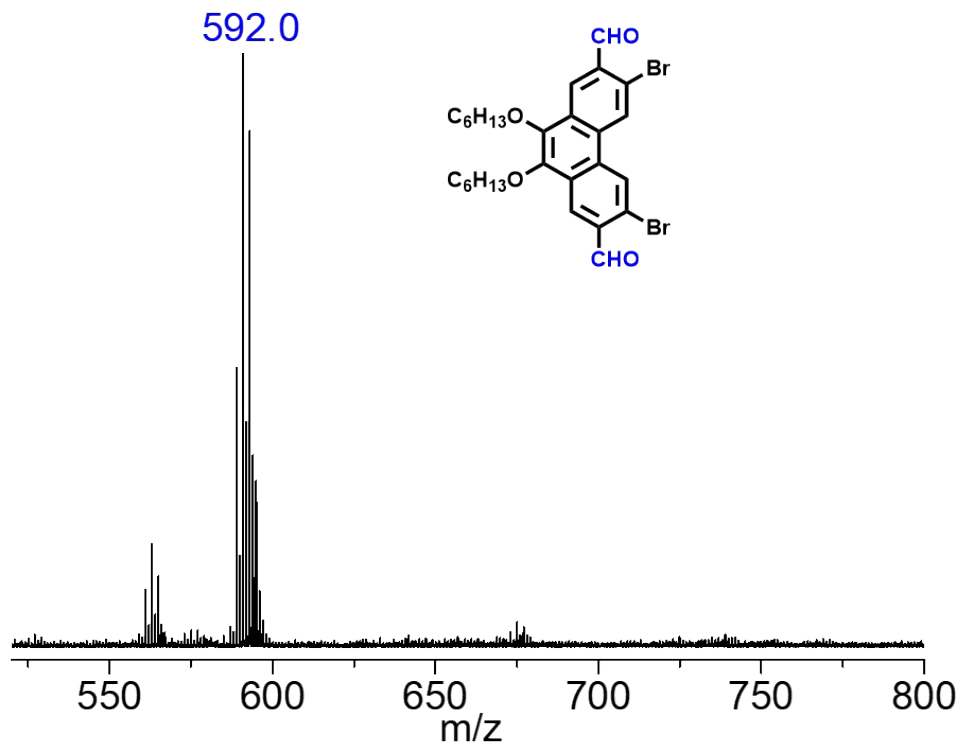


Figure S21. MALDI-TOF mass spectrum data for compound 1.

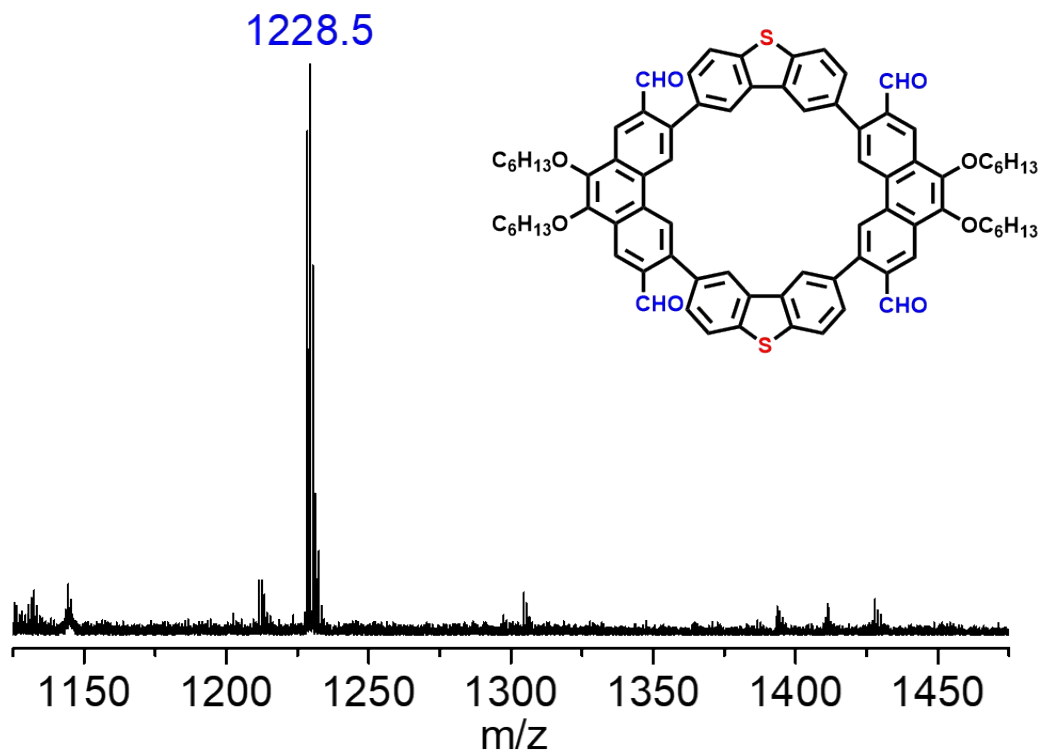


Figure S22. MALDI-TOF mass spectrum data for compound 3.

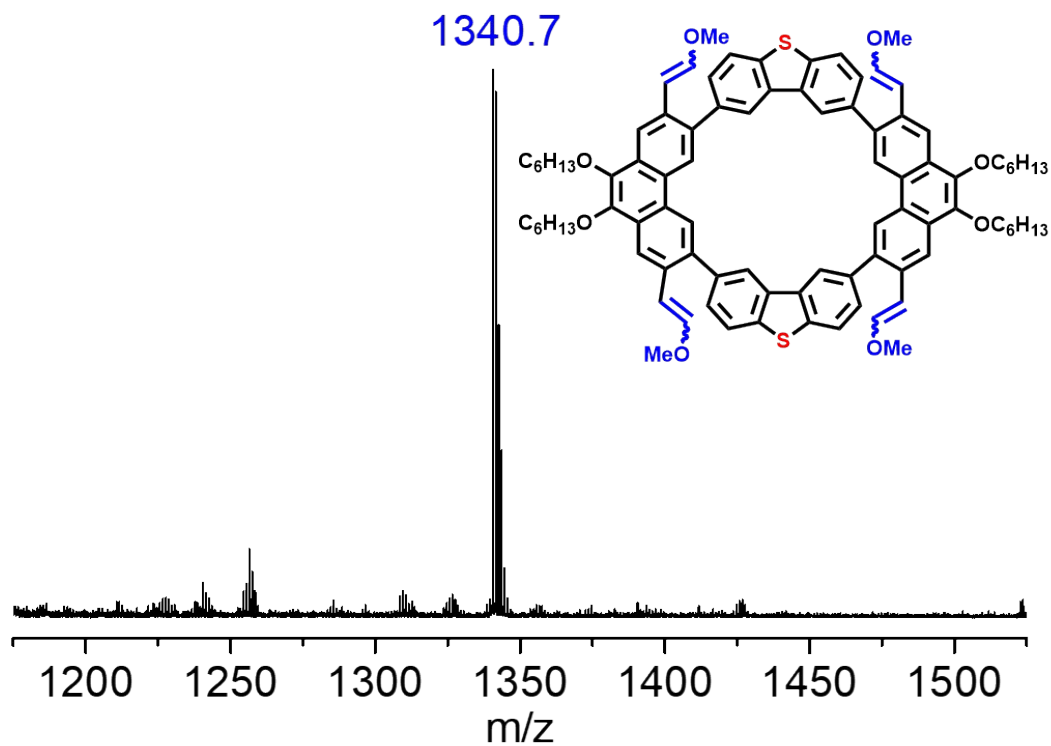


Figure S23. MALDI-TOF mass spectrum data for compound 4.

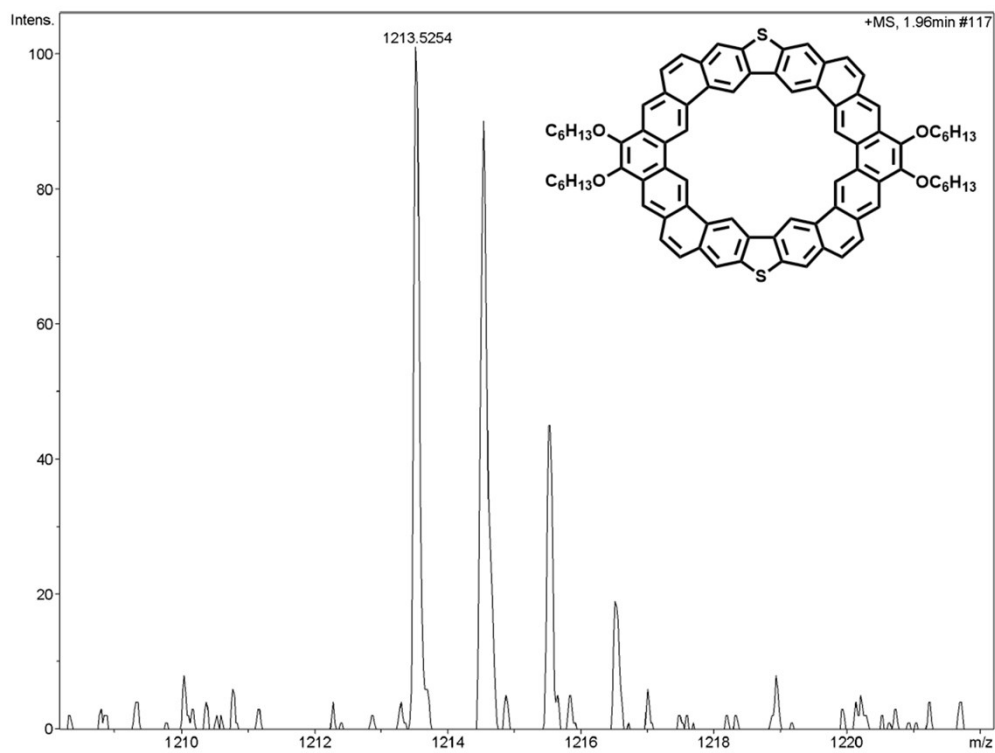


Figure S24. HR mass spectrum (APCI) of S-Octulene.

5. References

1. M. A. Majewski, Y. Hong, T. Lis, J. Gregoliński, P. J. Chmielewski, J. Cybińska, D. Kim, M. Stępień, *Angew. Chem. Int. Ed.* **2016**, *55*, 14072
2. S. M. Kim, J. H. Kim, S. K. Jeon, J. Y. Lee, *Dyes and Pigments*, **2016**, *125*, 274.
3. Gaussian 16, Revision A.03, M. J. Frisch, G. W. Trucks, H. B. Schlegel, G. E. Scuseria, M. A. Robb, J. R. Cheeseman, G. Scalmani, V. Barone, G. A. Petersson, H. Nakatsuji, X. Li, M. Caricato, A. V. Marenich, J. Bloino, B. G. Janesko, R. Gomperts, B. Mennucci, H. P. Hratchian, J. V. Ortiz, A. F. Izmaylov, J. L. Sonnenberg, D. Williams-Young, F. Ding, F. Lipparini, F. Egidi, J. Goings, B. Peng, A. Petrone, T. Henderson, D. Ranasinghe, V. G. Zakrzewski, J. Gao, N. Rega, G. Zheng, W. Liang, M. Hada, M. Ehara, K. Toyota, R. Fukuda, J. Hasegawa, M. Ishida, T. Nakajima, Y. Honda, O. Kitao, H. Nakai, T. Vreven, K. Throssell, J. A. Montgomery, Jr., J. E. Peralta, F. Ogliaro, M. J. Bearpark, J. J. Heyd, E. N. Brothers, K. N. Kudin, V. N. Staroverov, T. A. Keith, R. Kobayashi, J. Normand, K. Raghavachari, A. P. Rendell, J. C. Burant, S. S. Iyengar, J. Tomasi, M. Cossi, J. M. Millam, M. Klene, C. Adamo, R. Cammi, J. W. Ochterski, R. L. Martin, K. Morokuma, O. Farkas, J. B. Foresman, and D. J. Fox, Gaussian, Inc., Wallingford CT, **2016**.
4. (a) A. D. Becke, *J. Chem. Phys.* **1993**, *98*, 5648. (b) C. Lee, W. Yang, R. G. Parr, *Phys. Rev. B: Condens. Matter* **1988**, *37*, 785. (c) T. Yanai, D. Tew, N. Handy, *Chem. Phys. Lett.* **2004**, *393*, 51. (d) R. Ditchfield, W. J. Hehre, J. A. Pople, *J. Chem. Phys.* **1971**, *54*, 724. (e) W. J. Hehre, R. Ditchfield, J. A. Pople, *J. Chem. Phys.* **1972**, *56*, 2257. (f) P. C. Hariharan, J. A. Pople, *Theor. Chim. Acta* **1973**, *28*, 213.
5. (a) Z. Chen, C. S. Wannere, C. Corminboeuf, R. Puchta, P. v. R. Schleyer, *Chem. Rev.* **2015**, *105*, 3842. (b) H. Fallah-Bagher-Shaidaei, S. S. Wannere, C. Corminboeuf, R., Puchta, P. V. R. Schleyer, *Org. Lett.* **2006**, *8*, 863.
6. T. Lu, F. Chen, *J. Comput. Chem.* **2012**, *33*, 580.
7. D. Geuenich, K. Hess, F. Köhler, R. Herges, *Chem. Rev.* **2005**, *105*, 3758.